Topological sectors and the pion mass

S. Elser [*] and B. Bunk [†]

Institut für Physik, Humboldt–Universität, Invalidenstr.110,
10115 Berlin, Germany

February 1, 2008

Abstract

We study quenched and dynamical pion correlators in the two-flavour Schwinger model (2D QED) both within topological charge sectors and averaged. The results show that a clean-cut definition of a pion mass is no longer possible if tunneling between sectors does not occur.

PACS numbers: 11.15.Ha, 12.20.-m, 11.10.Kk

1   Introduction

Constructing decorrelated configurations in lattice simulations can be difficult if large energy barriers exist between regions of the configuration space to be sampled. One such possibility are topological sectors for the $U(1)$ model. While local updates do not work well, we can use in two dimensions a global heatbath update to obtain reasonably high tunneling rates. This trick obviously works also in the quenched case, while for full dynamical simulations global heatbath updates are not known yet.

A way of dealing with such systems which is sometimes suggested [1] is to stay in one fixed topological charge sector and define quantities in that way. In order to study this for relevant observables, we measure pion correlators for the massive two-flavour Schwinger model (QED in two dimensions) [2] in fixed (low) topological sectors. In the quenched case we compare local and global update schemes. For dynamical fermions we compare low and high β results, using both the local bosonic algorithm (LBA) [3] and Hybrid Monte Carlo (HMC) [4].

[*]supported by DFG research grant No. WO 389/3-2; email: elser@linde.physik.hu-berlin.de
[†]email: bunk@linde.physik.hu-berlin.de

2 Model

The use of the Schwinger model with two degenerate flavours of Wilson fermions is motivated by the fact that it is rather QCD-like, but still tractable with small computational effort. It exhibits an axial vector anomaly, light pseudoscalar mesons (pions) and massive particles (a_0, η) [5].

The lattice model is defined via the action

$$
\begin{aligned}
S &= S_G(U) + S_F(U, \Psi), \\
S_G &= \beta \sum_P (1 - \mathrm{Re}\, U_P), \\
S_F &= \sum_x \Big[\bar{\Psi}_x \Psi_x - \kappa \sum_\mu \Big(\bar{\Psi}_x(1 + \gamma_\mu) U_{x-\mu,\mu} \Psi_{x-\mu} + \bar{\Psi}_x(1 - \gamma_\mu) U^\dagger_{x,\mu} \Psi_{x+\mu} \Big) \Big],
\end{aligned}
$$

where S_G is the standard plaquette part and S_F the Wilson fermion action. U_P denotes the plaquette variable, $U_{x,\mu}$ the compact link at site x in direction μ and Ψ the two-component fermion field. We use periodic boundary conditions for link variables and anti-periodic ones for fermions throughout.

3 Algorithm

Quenched case: local update. We use a local link update consisting of one exact heatbath [6] and three over-relaxation steps per trajectory.

Quenched case: global update. Alternatively, it is possible to use a global heatbath for the plaquettes. As the new configuration is constructed without recursion to the old one, we expect to encounter much less problems with metastabilities. The global update uses the fact that nearly all plaquettes are independent even on a finite lattice. The plaquettes have only to satisfy the constraint

$$
\sum_P U_P = 2\pi n; \quad n \in \mathbb{Z}.
$$

We are therefore able to update $LT - 1$ plaquettes with a heatbath algorithm and then choose the last one using a Metropolis acceptance step. This plaquette configuration has to be translated into a valid link configuration. To achieve this, we utilize the freedom to choose a gauge. In our case we use a maximal tree prescription, setting $LT - 2$ links to 1. Then LT links can be recursively fixed from the plaquettes. The unconstrained two remaining links correspond to the free Polyakov loops P_T and P_L in 2 dimensions.

We want to state that the problem of slow topological charge fluctuations could also be solved by explicit topological updates [7]. Unfortunately, this trick is not applicable in the presence of dynamical fermions.

Full dynamical simulations. In this case we use the Hermitean version of Lüscher's local bosonic algorithm (LBA) [3]. A noisy Metropolis step is used to make the algorithm exact as described in [8, 9]. To have an independent check we have also implemented a Hybrid Monte Carlo (HMC) algorithm.

4   Topological sectors

The integer-valued topological charge functional

$$\frac{e}{4\pi} \int d^2x \epsilon_{\mu\nu} F_{\mu\nu}$$

can be represented on the lattice by

$$Q = \frac{1}{2\pi} \sum_P \phi_P$$

with plaquette angle $\phi_P = \text{Im} \ln(U_P) \in (-\pi, \pi)$ [10]. We denote by tunnel events all updates resulting in a change of the topological charge and as tunnel probability the number of tunnel events divided by the total number of updates. The topological susceptibility is defined via

$$\chi_{\text{top}} = \frac{1}{N_P}[< Q^2 > - < Q >^2].$$

We demonstrate the relevance of topological sectors on a 16×32 lattice showing in Fig. 1 the tunnel rate plotted against β for local and global updates. The exponential decrease of the tunnel probability for this local update algorithm gives rise to metastabilities in simulations at large β. We therefore consider it worthwile to investigate observables within fixed topological sectors.

5   Simulations

Simulation parameters. We simulate on 8×20 and 16×40 lattices at a beta value of $\beta = 12$ generating 10000 configurations. We only show data for the larger 16×40 lattices. For the fermion part, we choose $\kappa = 0.24$ where the pion correlation length (in the quenched case) is found to be around 3 and finite size effects can be expected to be small.
Local updates. We monitor the topological charge during our simulations. Due to metastability, no tunneling of Q is observed in the runs with local updates. At $\beta = 12$ we therefore are able to perform a simulation in a given topological

Figure 1: Tunnel probability as a function of β

U(1) pure gauge model   16x32
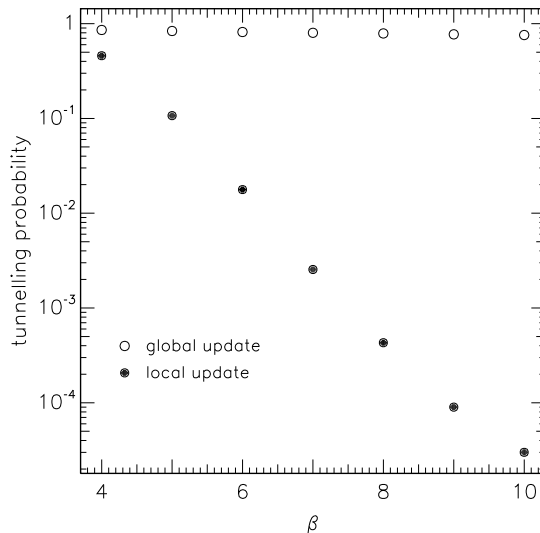
sector by using an initial configuration with this particular charge. This is done generating a classical homogeneous plaquette configuration of the desired charge and converting this to the links as described in Sect. 2. The two Polyakov loops P_T, P_L are chosen according to a flat random distribution.

Global updates. In the limit of independent plaquettes the topological susceptibility can be calculated analytically. An approximation for $\beta \to \infty$ gives

$$\chi_{\text{top}} \approx \frac{1}{4\pi^2\beta}.$$

which for $\beta = 12$ amounts to $\chi_{\text{top}} = 0.0022$. To check our global update, we simulate on a 16×32 lattice obtaining $\chi_{\text{top}} = 0.0021(1)$. This shows that the global update works well without metastabilities in the topological charge.

Observables. We measure the pion correlator using the operator $\bar{\psi}\gamma_5\tau\psi$. We apply a point source and wall sink prescription to increase statistics [8]. The effective masses are calculated from two adjacent time slices using the hyperbolical cosine formula. The error analysis of the effective pion mass takes covariances and auto-correlations of the correlators into account.

5.1   Quenched results

The results of the quenched runs are shown in Fig. 2.   Obviously, for $Q = 0, 4$ we are not able to find a plateau in the effective mass plots. We find a valley-like structure in the mass for the low Q cases. For high Q this turns into a hill-like

4

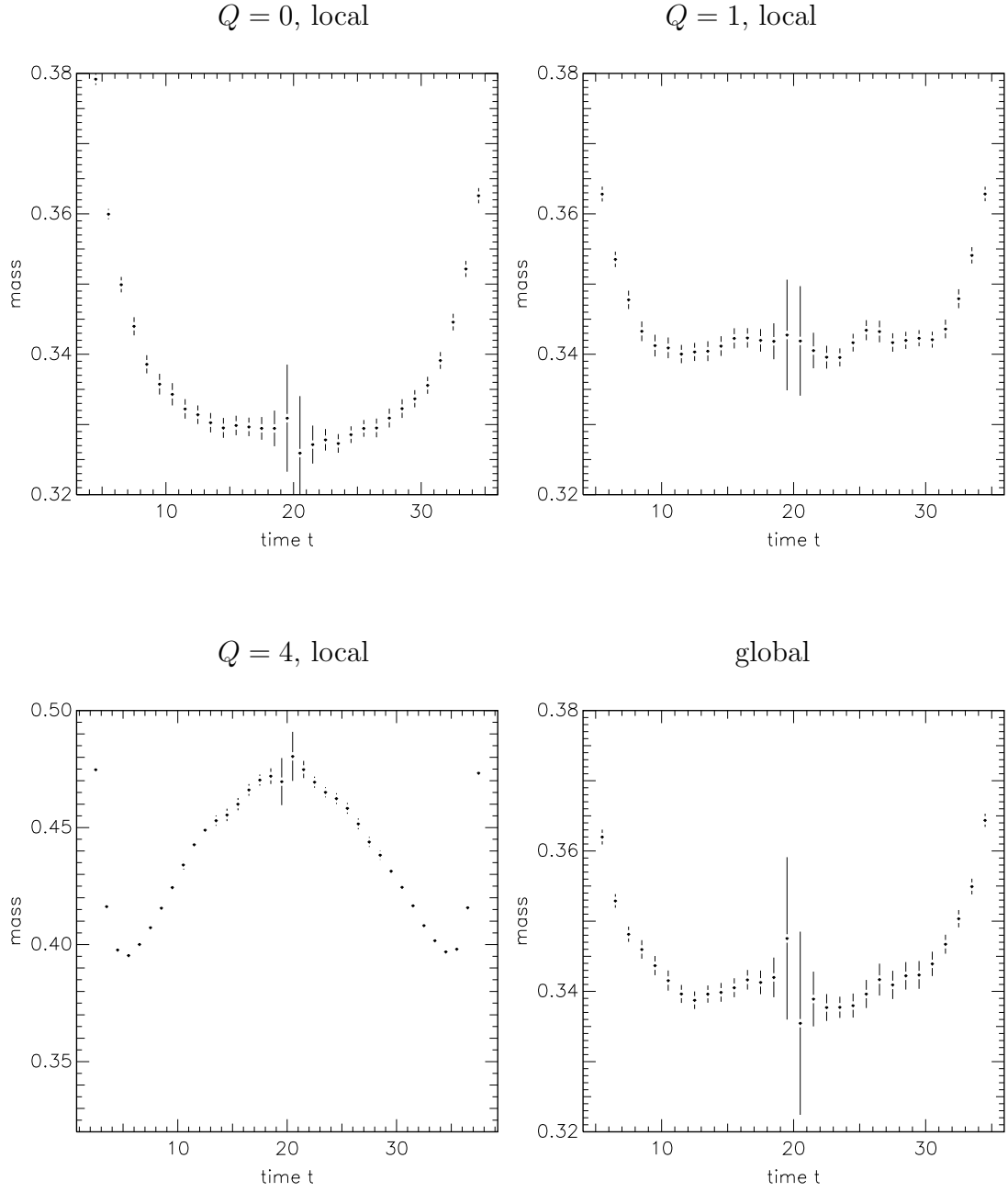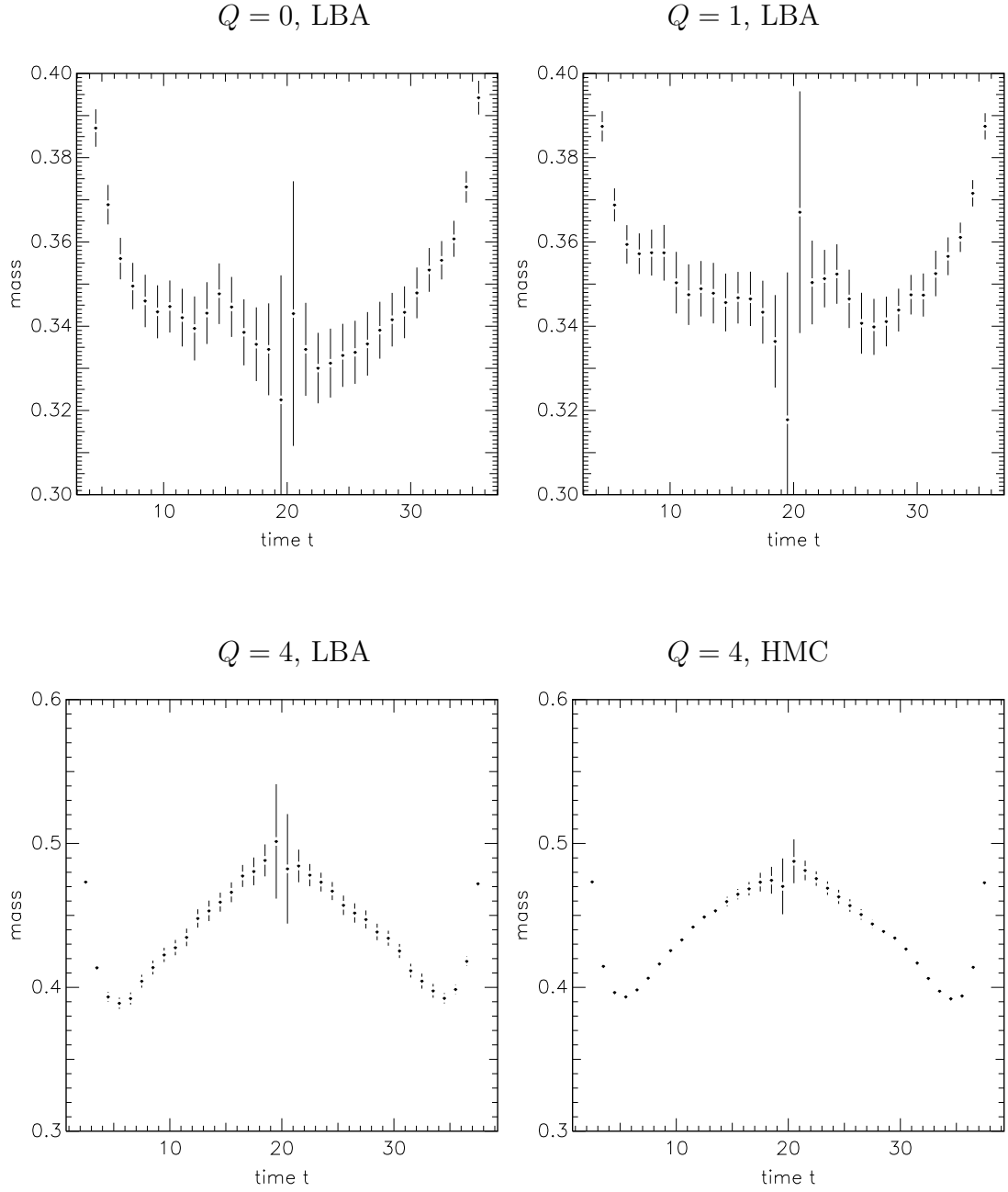Figure 2: Quenched effective pion mass as a function of time for $\beta = 12.0$, $\kappa = 0.24$

$Q = 0$, local

$Q = 1$, local

$Q = 4$, local

global

Figure 3: Dynamical effective pion mass as a function of time for $\beta = 12.0$, $\kappa = 0.24$

$Q = 0$, LBA

$Q = 1$, LBA

$Q = 4$, LBA

$Q = 4$, HMC

structure with the peak situated at half of the temporal lattice extent. To show that in the intermediate region the valley and hill structures can approximately cancel and suggest a fake plateau, we include the $Q = 1$ plot.

In the quenched case, we are able to compare to the results using a global update scheme. For the global update we find a tunnel probability of $P = 0.76$ and therefore do not expect any influence of topology. The effective mass is shown in Fig. 2d. A plateau is clearly more reasonable than in the fixed Q cases.

5.2 Dynamical fermion results

Effective masses from full dynamical simulations are shown in Fig. 3. We do not expect quantitatively the same results as in the quenched case. But the behaviour is qualitatively similar.

To establish that our dynamical results are not influenced by the chosen parameters of the local bosonic algorithm, we repeat the calculation with topological charge $Q = 4$ using a standard HMC algorithm. This is also shown in Fig. 3. The results agree nicely within errorbars.

From these results, we conclude that we need to average over the topological sectors to obtain a plateau in the effective mass.

6 Projections to topological sectors

To gain further insight, we now use a slightly different approach. In principle, we could also restrict ourselves to definite topological sectors by selecting measurements with fixed topological charge from a simulation, i.e. effectively simulating the path integral given by

$$Z[q] = \int D[U]D[\bar{\Psi}]D[\Psi]\delta_{Q,q}e^{-S}.$$

To this end we need simulations with a reasonably high fluctuation. Such simulations can be done e.g. with dynamical simulations at low β or quenched simulations using global updates.

Full dynamical case. We work at low $\beta = 1$ with a slightly smaller $\kappa = 0.22$. Effective masses are depicted in Fig. 4. We can detect no discrepancy between masses calculated in different topological sectors. This result was also reported by a group working with staggered fermions, which concluded that topological sectors to not matter for the Schwinger model [1].

Quenched case. Here we exploit the opportunity to use the same parameters $\beta = 12, \kappa = 0.24$ as in Sect. 5. The results are shown in Fig. 5. At this β, we do

Figure 4: Dynamical projected effective pion mass as a function of time for $\beta = 1.0$, $\kappa = 0.22$
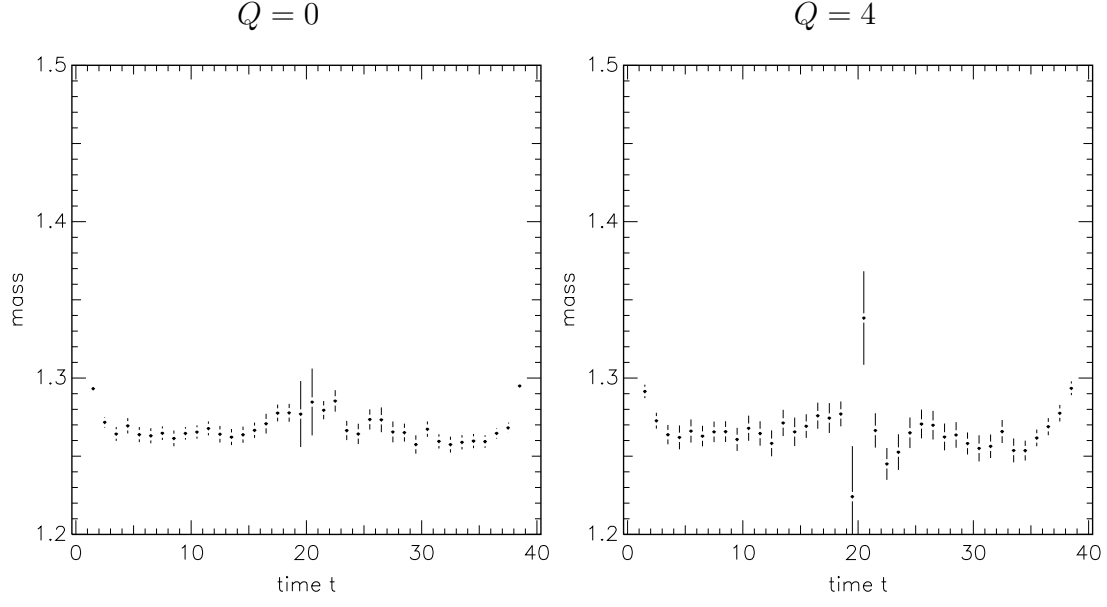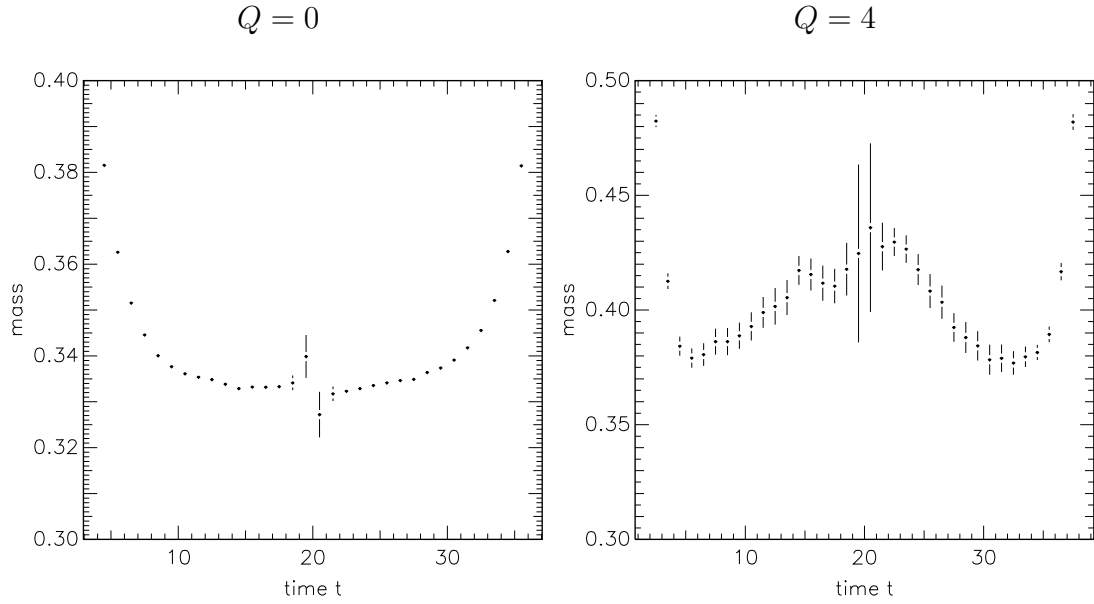

Figure 5: Quenched projected effective pion mass as a function of time for $\beta = 12.0$, $\kappa = 0.24$

not find agreement. Rather the effective masses are nearly the same as in the simulations without tunneling presented in Fig. 3. We would like to point out that they do not agree within errorbars. On the other hand, we remark that the statistical sample was very much smaller for the projected data due to the fact that only a part of the generated configurations is projected into the appropriate sectors.

The striking difference between low and high β results makes a sound understanding of this behaviour highly desirable. It is evidently not just the averaging over the topological sectors (as found in Sect. 5) which is lacking in high β simulations, but there seems to be some more subtle dynamical effect involved.

7   External gauge configurations

In order to further investigate how much averaging is necessary we plot in Fig. 6 effective masses for external configurations with fixed topological charge $Q = 0$ and $Q = 4$. These are generated from homogeneous plaquette configurations in the way described in Sect. 2. For the fermions we use $\kappa = 0.24$.

We stress that we use random Polyakov loops P_T, P_L in both cases, so that one should not expect free fermion behaviour in the $Q = 0$ case. For $Q = 4$ a completely irregular behaviour is observed. It is thus not possible to measure a meaningful pion correlator from one (even very smooth) configuration alone. The translation invariance is manifestly broken even for that smooth configuration.

The result of averaging over 10 values of P_T and P_L is shown in Fig. 7. We clearly regain the qualitatively expected regular valley and hill structure observed in Fig. 3 in both the $Q = 0$ and $Q = 4$ case.

8   Conclusion

Our results for effective pion masses for simulations at fixed topological charge at high β clearly show that definition of a pion mass from a plateau is not possible for both quenched and dynamical simulations even for vanishing topological charge. A comparison with quenched global updates exhibiting no metastabilities demonstrates that a plateau can be found in the correct path integral sample. Furthermore, cross-checks against HMC indicate that this problem is not an artifact stemming from the fermion algorithm.

In Sect. 6, we studied effective pion masses calculated from projections to fixed topological sectors. Results from fluctuating ensembles show no dependence on

Figure 6: Effective pion mass as a function of time from one external configuration at $\kappa = 0.24$
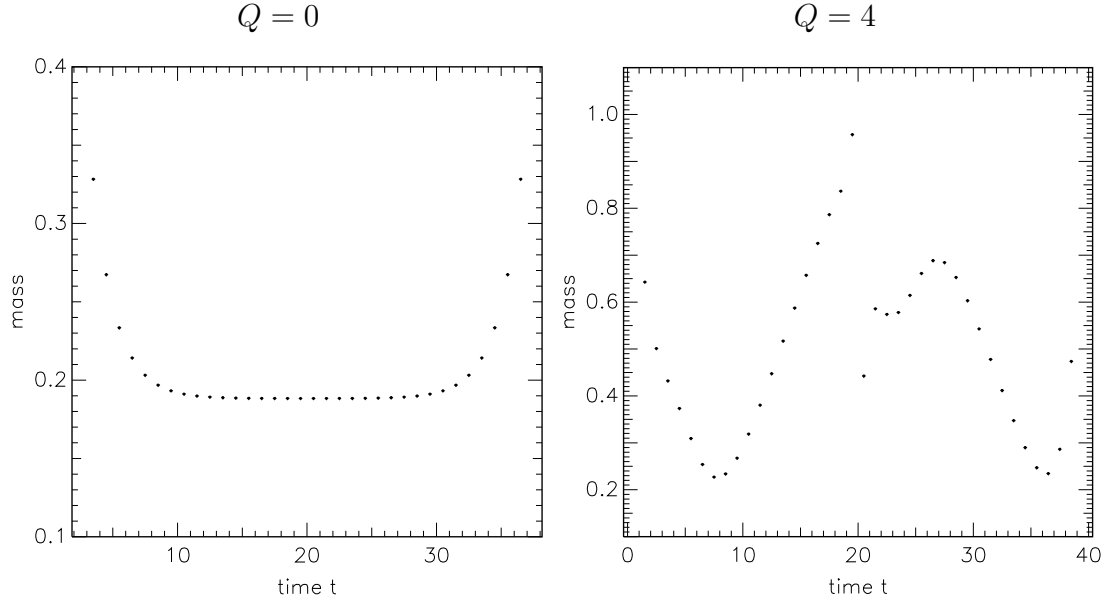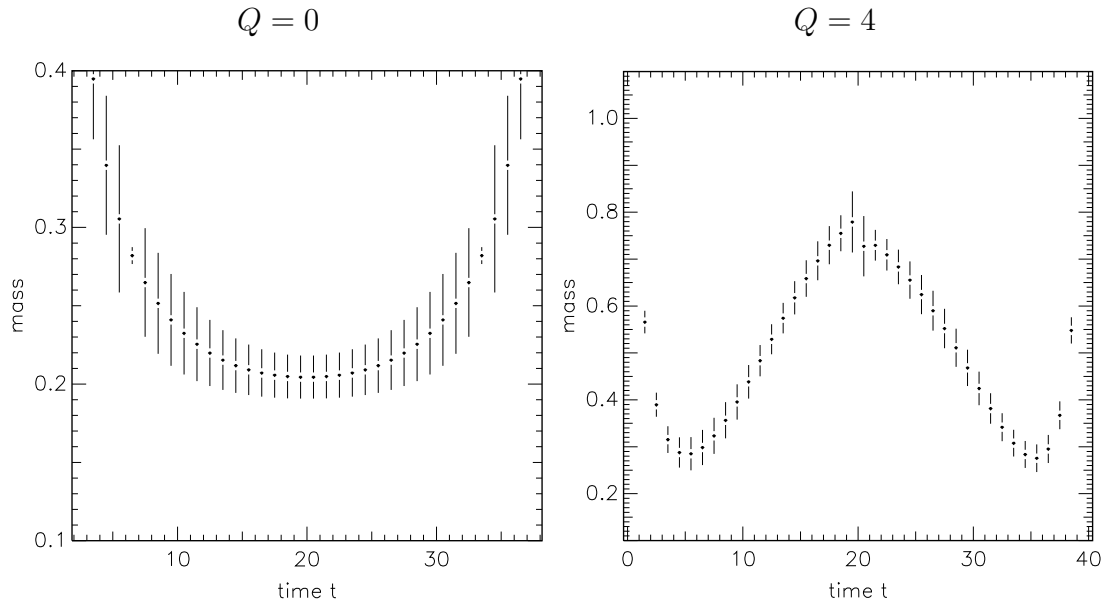
$Q = 0$

$Q = 4$

Figure 7: Effective pion mass as a function of time from ten external configurations at $\kappa = 0.24$

$Q = 0$

$Q = 4$

the topological charge. On the other hand, those projected from non-fluctuating ensembles show approximately the same behaviour as simulations completely without tunneling. This suggests a rather subtle dynamical effect.

In Sect. 7 we found that external homogeneous plaquette configurations with fixed Polyakov loop values P_T and P_L exhibit completly irregular behaviour. After averaging over P_T and P_L we regain the effective mass results characteristic for the topological charge sectors these configurations lie in.

We conclude that there is a need to obtain a better understanding of the interplay between the dynamical mass generation and topological sectors. We would like to point out that higher statistics runs could reveal similar phenomena in other models with non-trivial topological structure.

9   Acknowledgements

References

[1] C. Gutsfeld, H.A. Kastrup, K. Stergios, J. Westphalen, hep-lat/9709158

[2] J. Schwinger, Phys. Rev. 128 (1962) 2425.

[3] M. Lüscher, Nucl. Phys. B418 (1994) 637.

[4] S. Duane, A.D. Kennedy, B.J. Pendleton, D. Roweth, Phys. Lett. B195 (1987) 216.

[5] J.E. Hetrick, Y. Hosotani, S. Ito, Phys. Rev. D53 (1996) 7255,
Phys. Lett. B350 (1995) 92.

[6] D.J. Best, N.I. Fisher, Appl. Statist. 28 (1979) 152.

[7] H. Dilger, Nucl. Phys. B 434 (1995) 321,
Int. Jour. Mod. Phys. C6 (1995) 123

[8] S. Elser and B. Bunk, Nucl. Phys. B (proc. Suppl.) 53 (1997) 953

[9] S. Elser and B. Bunk, hep-lat 9709121,
to appear in the proceedings of Lattice97.

[10] M. Lüscher, Commun. Math. Phys. 85 (1982) 39.